Theoretical Chemistry Accounts (2019) 138:125
https://doi.org/10.1007/s00214-019-2512-4

REGULAR ARTICLE

Excited state intramolecular proton transfer via different size of hydrogen bond ring: a theoretical insight

Mei Ni[1] · Shenyang Su[1] · Hua Fang[1]

Received: 9 June 2019 / Accepted: 14 November 2019 / Published online: 20 November 2019

Abstract

4′-methoxy-3-hydroxyflavone (5-HB), 2-(5-carboxyphenyl)-2-hydroxyphenyl) benzothiazole (6-HB) and *o*-LHBDI (7-HB), which have five-, six- and seven-membered intramolecular H-bonding ring between proton donor and proton acceptor, respectively, were chosen to investigate excited state intramolecular proton transfer (ESIPT) process in the gas phase by using density functional theory and time-dependent density functional theory methods. The intramolecular H-bond is strengthened in the excited state on account of the structural parameters and IR vibrational frequencies of the related group. The enhanced intramolecular H-bond is favorable of ESIPT process to convert enol form into keto form. 7-HB has a high chemical activity and low kinetic stability by analyzing the energy gap between the highest occupied molecular orbital and the lowest unoccupied molecular orbital. The calculated absorption and fluorescence spectra are in agreement with the experimental values. The potential energy curves (PECs) of 5-HB, 6-HB and 7-HB in the S_0 and S_1 states are scanned by altering O_1–H_2 distance in increment of 0.05 Å. Our PECs results indicate that ESIPT happens easily in the S_1 state with a very small barrier. The rate of ESIPT process follows this order: 6-HB~7-HB > 5-HB.

Keywords Excited state intramolecular proton transfer · Hydrogen bond · Electronic spectra · Potential energy curve

1 Introduction

Proton transfer (PT) plays a significant part in all sorts of chemical and biological systems [1–6]. Proton transfer can happen in the ground or excited state. From the viewpoint of photochemistry, the excited state proton transfer (ESPT) and excited state intramolecular proton transfer (ESIPT) begin with photoexcitation, in which the driving force based on acidity or basicity is strengthened, and then, PT occurs. In recent years, researchers have developed the application of ESIPT molecules and found them to be extremely powerful application value in light stabilizers [7], laser fuels [8], photoexcited materials [9], light-emitting materials in luminescent devices [10], fluorescent probes [11] and biological systems [12]. ESIPT molecule also can be applied to be a preferred material for photonic devices such as optical switches, optical limiting, optical waveguides and real-time optical storage. Studying the ESIPT reaction is of great significance for photochemical and photobiological processes and thus has become one of the hotspots of experimental and theoretical researches in the chemical field [13–15].

ESPT takes place from the proton donor to the proton acceptor among different molecules by forming dimers or complexes via intermolecular hydrogen-bonding (H-bonding). ESIPT is a single molecular reaction. Since the proton donor and acceptor are present in the same molecule and have a suitable distance, the proton transfer process can be accomplished with the aid of intramolecular H-bonding. Hence, the formation of intramolecular H-bond is a necessary step for proton transfer in the excited state. Most of the ESIPT systems involve hydroxyl or amino groups serving as the proton donors and carbonyl oxygen or azo nitrogen serving as the proton acceptors. Along the intramolecular H-bonding, a five-, six-, seven- or even eight-membered ring structure can be formed between proton donor and proton acceptor. In other words, at least a five-membered ring can undergo ESIPT [16–24].

ESIPT reaction is a four-level photoinduced tautomerism process. Generally, ESIPT molecule in its enol (*E*) form is the most stable in the ground state (S_0), whereas its

✉ Hua Fang
susanfang20@gmail.com

[1] Department of Chemistry and Material Science, College of Science, Nanjing Forestry University, Nanjing 210037, People's Republic of China

keto (*K*) form is more stable in the first singlet excited state (S_1). Upon photoexcitation, the enol (*E*) structure should be excited to the excited state form (E^*), and then, a proton can migrate from donor to acceptor with the structure transformation from E^* to K^*. After intense fluorescence emission from K^* to *K* with a large Stokes shift (up to 10,000 cm^{-1}), *K* structure returns back to the *E* structure via ground state intramolecular proton transfer (GSIPT) to accomplish the four-level process [25–29].

Most ESIPT processes have much less barrier height due to the strong intramolecular H-bond in ESIPT compound. The close distance between proton donor and proton acceptor in the ESIPT molecule is important to the ESIPT process [30, 31]. Namely, the strength of intramolecular H-bond has crucial effect on the photophysical properties of the ESIPT rate. Proton transfer reactions usually happen via forming a six-membered ring with a strong intramolecular H-bond between the proton donor and acceptor [32–43]. ESIPT occurring in five-membered [44–46] and seven-membered [17, 47] systems is not common. The H-bond distance in the five-, six- and seven-membered ring varies on sub-angstrom scale with their ESIPT ability [48]. On account of the previous studies, the subtle changes of H-bond distance may result in distinct effect on the fluorescence properties [8]. However, no systematical theoretical studies on five-, six- and seven-membered ring H-bonding systems have been reported. In this respect, it is very significant to research the ESIPT process of the five-, six- and seven-membered ring H-bonding systems, which is meaningful to interpret biochemical phenomena and design new ESIPT molecules.

A representative five-membered ring intramolecular H-bond system undergoing ESIPT process is 3-hydroxyflavone (3HF) derivatives. The emitting fluorescence properties of 3HF are very sensitive to H-bonding perturbations [49], and the intramolecular H-bond strength of 3HF can be tuned by adjusting the pi electron system conjugation through the two rings of the molecule. Sholokh et al. [50] synthesized a fluorescent L-amino acid containing 4′-methoxy-3-hydroxyflavone fluorescent group, which has a methoxy group in the para-position on the 2-phenyl moiety and exhibits double emission due to ESIPT. Another classical ESIPT molecule is 2-(2-hydroxyphenyl) benzothiazole (HBT), which has a six-membered intramolecular H-bond ring between proton donor (–OH) and proton acceptor (–N=). HBT and its derivatives are organic light-emitting and fluorescent probing materials and can occur ESIPT process in hundreds femtoseconds [51, 52]. Recently, a new compound of 2-(5-(4-carboxyphenyl)-2-hydroxyphenyl) benzothiazole was designed and synthesized by Li et al. based on the HBT form [53]. In contrast to a large number of studies on six-membered H-bonding ESIPT molecule [32–43], studies on the seven-membered ring intramolecular H-bonding system are very rare because of the weaker H-bond strength [17–19, 54–57]. For the seven-membered ring H-bonding ESIPT molecule, a typical example is 4-(2-hydroxy-benzylidene)-1,2-dimethyl-1*H*-imidazol-5(4*H*)-one (*o*-HBDI), which has the similar structure to the core chromophore of green fluorescent protein [17]. Upon electronic excitation, *o*-HBDI takes place ESIPT and leads to a large Stokes-shifted tautomer emission at 605 nm. Recently, based on the rule that the quantum yield of fluorescence emission would be increased with the structural rigidity, a structurally locked *o*-HBDI core chromophore, *o*-LHBDI has been reported by Hsu et al. [56].

In this work, we employed the density functional theory (DFT) and time-dependent density functional theory (TDDFT) methods to systemically research the ESIPT processes of the typical five-, six- and seven-membered ring intramolecular H-bond molecules 4′-methoxy-3-hydroxyflavone (5-HB), 2-(5-(4-carboxyphenyl)-2-hydroxyphenyl) benzothiazole (6-HB) and *o*-LHBDI (7-HB) (see Fig. 1). The potential energy surfaces along the PT reactions both in the ground and excited states were described, and the structures, the barrier height of PT and spectral properties with vertical electronic absorption and emission were investigated. We hope that these detailed theoretical researches can throw a light on the correlation with the size of intramolecular H-bond and ESIPT mechanism.

2 Computational details

The structures of 5-HB, 6-HB and 7-HB were optimized in the gas phase by using DFT and TDDFT methods for the S_0 and S_1 states, respectively. The hybrid functional of Truhlar and Zhao [58] (M06-2X) and 6-31 + G(*d*,*p*) basis

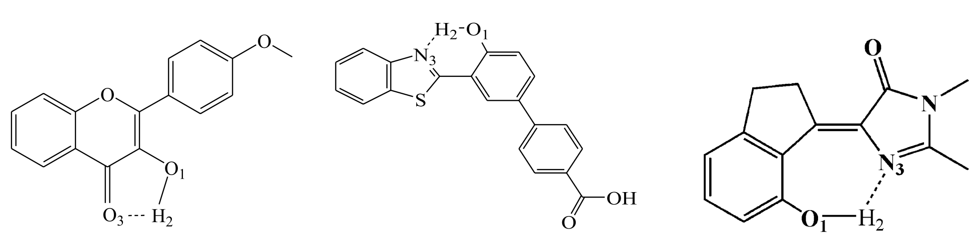

5-HB 6-HB 7-HB

Fig. 1 Enol structures of 5-HB, 6-HB and 7-HB set in the Gaussian 09 program [59] were employed. The frequency calculation has been carried out at the same computational level after the geometry optimization in order to testify the minima (reactant and product) and transition state (TS). Only one imaginary frequency and no imaginary frequency for the TS and minima along the potential surface of ESPT were found, respectively. The absorption and fluorescence spectra were performed at TD-M06-2X/6-31 + G(*d*,*p*) level with the S_0 and S_1 optimized structures. In order to deeply understand the ESIPT process, the S_0 and S_1 constrained potential energy curves (PECs) were scanned by point-to-point optimizations at M06-2X/6-31 + G(*d*,*p*) and TD-M06-2X/6-31 + G(*d*,*p*) levels, respectively. For each stationary point optimization, the reaction coordinate O_1–H_2 distance was fixed at a given range, while the other parameters are fully optimized without any constraint. Along the PECs, the increment of O_1–H_2 distance is 0.05 Å.

3 Results and discussion

3.1 Geometric structures

In this part, we studied the enol form structures of 5-HB, 6-HB and 7-HB first obtained by using M06-2X and TD-M06-2X methods in both S_0 and S_1 states, respectively. The optimized structural parameters related to the H-bonds of 5-HB, 6-HB and 7-HB in the ground (S_0) and excited states (S_1) are listed in Table 1. Based on our calculated results, the bond lengths of O_1–H_2, H_2–O_3 and O_1–O_3 of 5-HB are 0.976 Å, 2.032 Å and 2.632 Å in the S_0 state, respectively. After excitation to S_1 state, the corresponding bond distances are 0.998 Å, 1.838 Å and 2.535 Å, respectively. At the same time, the O_1–H_2–O_3 bond angle changes from 117.8° in the S_0 state to 124.0° in the S_1 state. With comparison to the corresponding values in the S_0 state, the bond length of O_1–H_2 in 5-HB increases by 0.022 Å in the S_1 state, but H_2–O_3 and O_1–O_3 distances shorten by 0.194 Å and 0.097 Å, respectively. In addition, the O_1–H_2–O_3 bond angle in the S_1 state increases by 6.2° than that value in the S_0 state. These results indicate that intramolecular H-bond H_2–O_3 is enhanced in the S_1 state. Similarly, the O_1–H_2 bond length of 6-HB elongates from 0.987 Å in the S_0 state to 1.063 Å in the S_1 state. On the contrary, H_2–N_3 and O_1–N_3 distances shorten 0.267 Å and 0.150 Å in the excited state, respectively. The O_1–H_2–N_3 bond angle of 6-HB in the S_1 state increases by 6.5°. In the 7-HB compound, the O_1–H_2, H_2–N_3 and O_1–N_3 bond distances in the S_1 state increase by 0.047 Å and decrease by 0.155 Å and 0.105 Å, respectively, compared to those values in the S_0 state. It is obvious that the H_2–N_3 intramolecular H-bonds of 6-HB and 7-HB in the S_1 state are stronger than those in the S_0 state. Moreover, H_2–N_3 H-bond distances of 7-HB and 6-HB in the S_1 state are with small difference, but both are much shorter than the corresponding H-bond of 5-HB, and the O_1–H_2–N_3 bond angle of 7-HB is much larger than those of 6-HB and 5-HB. All these results indicate that the intramolecular H-bond strengths of 7-HB and 6-HB in the S_1 state are stronger than that of 5-HB and is anticipated to promote the ESIPT process in 7-HB and 6-HB. Furthermore, simulating the infrared (IR) vibrational spectra of 5-HB, 6-HB and 7-HB may provide an effective way to further explain the changes of H-bond in the S_0 and S_1 states. As shown in Fig. 2 and Table 1, the calculated frequencies of O_1–H_2 stretching vibration of 5-HB, 6-HB and 7-HB are situated at 3702 cm^{-1}, 3358 cm^{-1} and 3057 cm^{-1} in the S_0 state, while

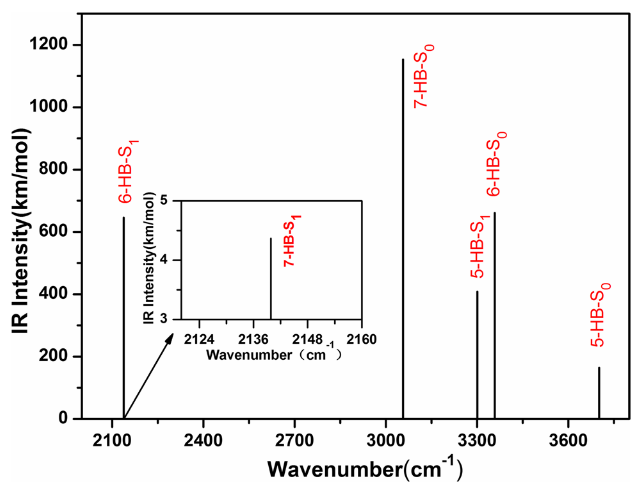

Fig. 2 IR spectra for 5-HB, 6-HB and 7-HB in the region of the O_1–H_2 stretching vibration frequencies in the S_0 and S_1 states at the M06-2X/6-31 + G(*d*,*p*) and TD-M06-2X/6-31 + G(*d*,*p*) levels

Table 1 Bond lengths (in Å), bond angles (in °) and IR vibrational frequencies of O_1–H_2 of the S_0 and S_1 states for the studied compounds 5-HB, 6-HB and 7-HB in gas obtained at the M06-2X/6-31 + G(*d*,*p*) and TD-M06-2X/6-31 + G(*d*,*p*) levels

	5-HB		6-HB		7-HB	
	S_0	S_1	S_0	S_1	S_0	S_1
O_1–H_2	0.976	0.998	0.987	1.063	1.003	1.050
H_2–N_3/O_3	2.032	1.838	1.759	1.492	1.633	1.478
O_1–N_3/O_3	2.632	2.535	2.631	2.481	2.620	2.515
$\delta(O_1–H_2–N_3/O_3)$	117.8	124.0	145.4	151.9	167.1	168.2
$\upsilon(O_1–H_2)$	3702	3300	3358	2138	3057	2140

3300 cm^{-1}, 2138 cm^{-1} and 2140 cm^{-1} in the S_1 state. It is worth noting that the 402 cm^{-1}, 1220 cm^{-1} and 917 cm^{-1} redshift of the O–H stretching frequency demonstrates that intramolecular H-bonding (O_1–H_2···O_3/N_3) is strengthened in the S_1 state.

3.2 Electronic spectra and frontier molecular orbitals

The first excited state structures of 5-HB, 6-HB and 7-HB compounds are completely optimized at TD-M06-2X/6-31 + G(*d*,*p*) level. The calculated absorption and fluorescence spectra of 5-HB, 6-HB and 7-HB compounds in the gas phase obtained at the TD-M06-2X/6-31 + G(*d*,*p*) level are displayed in Fig. 3. The optimized geometries in the S_0 and S_1 states are served as the initial structure to obtain the S_0–S_1 vertical excitation energy and electronic spectra. It can be found that the calculated absorption peak for 5-HB, 6-HB and 7-HB lies on 313.7 nm, 310.8 nm and 341.4 nm, which are consistent with experimental values (5-HB: 350–355 nm; 6-HB: 282–390 nm; 7-HB: ~ 380 nm) [50, 53, 56].

Moreover, the fluorescence properties of 5-HB, 6-HB and 7-HB are also simulated at the enol and keto forms. The calculated fluorescence emission peaks of 5-HB-enol and 5-HB-keto are situated at 360.1 nm and 491.6 nm, respectively, which are in agreement with the experimental data (enol form: 410–420 nm; keto form: 530–541 nm) [60]. Evidently, the emission peak of 5-HB-enol redshifts 46.3 nm compared to the absorption peak, which would be attributed to the Stokes shift, whereas the 5-HB-keto emission peak has a large redshift of 177.9 nm compared to the absorption peak. Similarly, for 6-HB and 7-HB, dual fluorescent emission peaks are obtained at 366.5 nm, 397.4 nm for enol form and 471.7 nm, 472.1 nm for the keto form, respectively. Our theoretical fluorescence emission peaks of 6-HB and 7-HB are consistent with the experimental values [6-HB: 398 nm (enol form), 540 nm (keto form); 7-HB: 480 nm (enol form), 585 nm

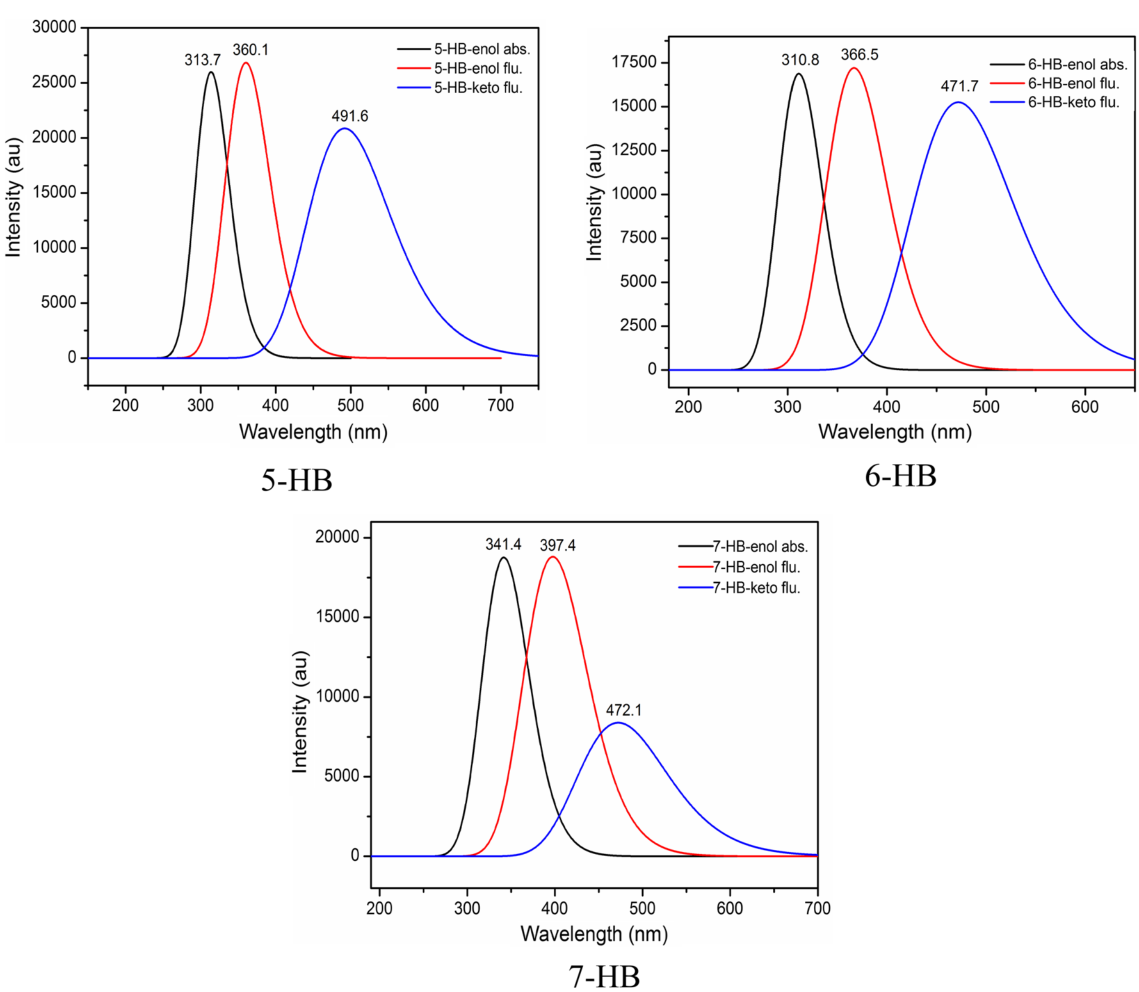

Fig. 3 Calculated absorption and fluorescence spectra of 5-HB, 6-HB and 7-HB in the gas phase at the TD-M06-2X/6-31 + G(*d*,*p*) level

(keto form)]. The fluorescence emission peaks exhibit the Stokes shift of 55.7 nm and 56.0 nm for the enol form of 6-HB and 7-HB molecules, respectively. In addition, the keto forms of 6-HB and 7-HB molecules have a large red-shift of 160.9 nm and 130.8 nm, respectively, between the fluorescent emission peak and the absorption peak. The double emission peaks mean that 5-HB, 6-HB and 7-HB molecules have two isomers (enol and keto) in the S_1 state, and the keto form isomer of 5-HB, 6-HB and 7-HB generated due to ESIPT process.

In order to explore the nature of the conformations of charge distribution in the S_1 state and ESIPT dynamics, the frontier MO of 5-HB, 6-HB and 7-HB in gas was analyzed and is shown in Fig. 4. Herein, the highest occupied molecular orbital (HOMO) and the lowest unoccupied molecular orbital (LUMO) are depicted in the S_1 state. From Fig. 4, it can be clearly seen that the HOMO and LUMO in the S_1 state have π and π^* character localized on different parts of 5-HB, 6-HB and 7-HB molecules, respectively, which demonstrates that the transition from the HOMO and LUMO is a predominant $\pi\pi^*$-type transition with a charge transfer character. It is worth noting that the charge densities of hydroxyl moiety (O_1–H_2) and proton acceptor (O_3/N_3) decrease and increase through the transition from HOMO to LUMO, respectively. According to valence bond theory, the added electron density of acceptor O_3/N_3 atoms would be of great importance in strengthening the intramolecular H-bond and then facilitates ESIPT [61–68]. The chemical activity of the molecule can be reflected by the energy gap between HOMO and LUMO. The high chemical activity and low kinetic stability mean a small energy gap [69, 70]. The energy gaps of 5-HB, 6-HB and 7-HB compounds are 5.20 eV, 5.36 eV and 4.99 eV, respectively. The energy gap of 7-HB is smaller than those of 5-HB and 6-HB, meaning that 7-HB has a high chemical activity and low kinetic stability. Namely, it is much easier to occur ESIPT process for 7-HB compound.

3.3 Potential energy curves

In order to better understand the ESIPT processes of 5-HB, 6-HB and 7-HB molecules, we constructed the potential energy curves (PECs) in the S_0 and S_1 states by M06-2X/6-31 + G(d,p) and TD-M06-2X/6-31 + G(d,p) methods, respectively. Potential energy curves are scanned by using the constrained optimizations in the S_0 and S_1 states with fixed O_1–H_2 distance in a given range and in increments of 0.05 Å. The range of O_1–H_2 distance in PEC was selected because all the enol, transition state and keto structures can be contained in it. The information of qualitative energetic pathways for the ESIPT process can be obtained by PECs.

As shown in Fig. 5, the relative energy of 5-HB, 6-HB and 7-HB in the S_0 state is lower than that in the S_1 state, which means that the enol form of 5-HB, 6-HB and 7-HB compounds in the S_1 state is unstable and ESIPT process is apt to happen by crossing a small barrier (1.87 kcal/mol for 5-HB, 0.23 kcal/mol for 6-HB and 0.34 kcal/mol for 7-HB). In addition, the reverse ESIPT barriers are 10.9 kcal/mol, 4.73 kcal/mol and 1.42 kcal/mol for 5-HB, 6-HB and 7-HB, respectively, and all the barriers are bigger than ESIPT barriers, demonstrating that 5-HB, 6-HB and 7-HB in the S_1 state exist in the keto forms. It can also be seen that no stationary points for 6-HB and 7-HB-keto forms in the ground state can be obtained, which indicates that proton transfer processes cannot occur. The proton transfer is also hard to proceed for the enol forms of 5-HB molecule in the S_0 state to turn in the keto forms because of the relatively high barrier (5-HB: 16.0 kcal/mol) and endothermic reaction. On the contrary,

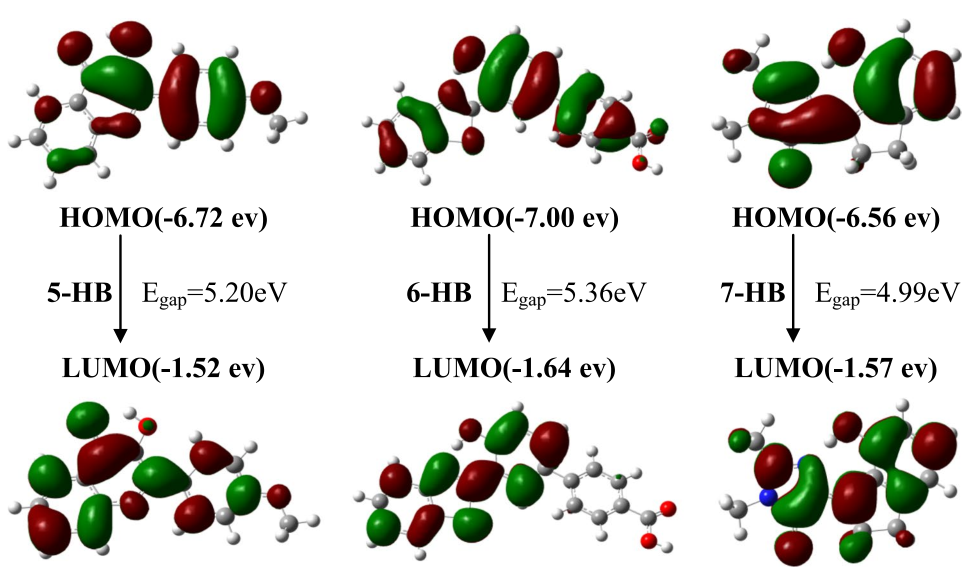

Fig. 4 Frontier molecular orbitals (HOMO and LUMO) of 5-HB, 6-HB and 7-HB in the S_1 state

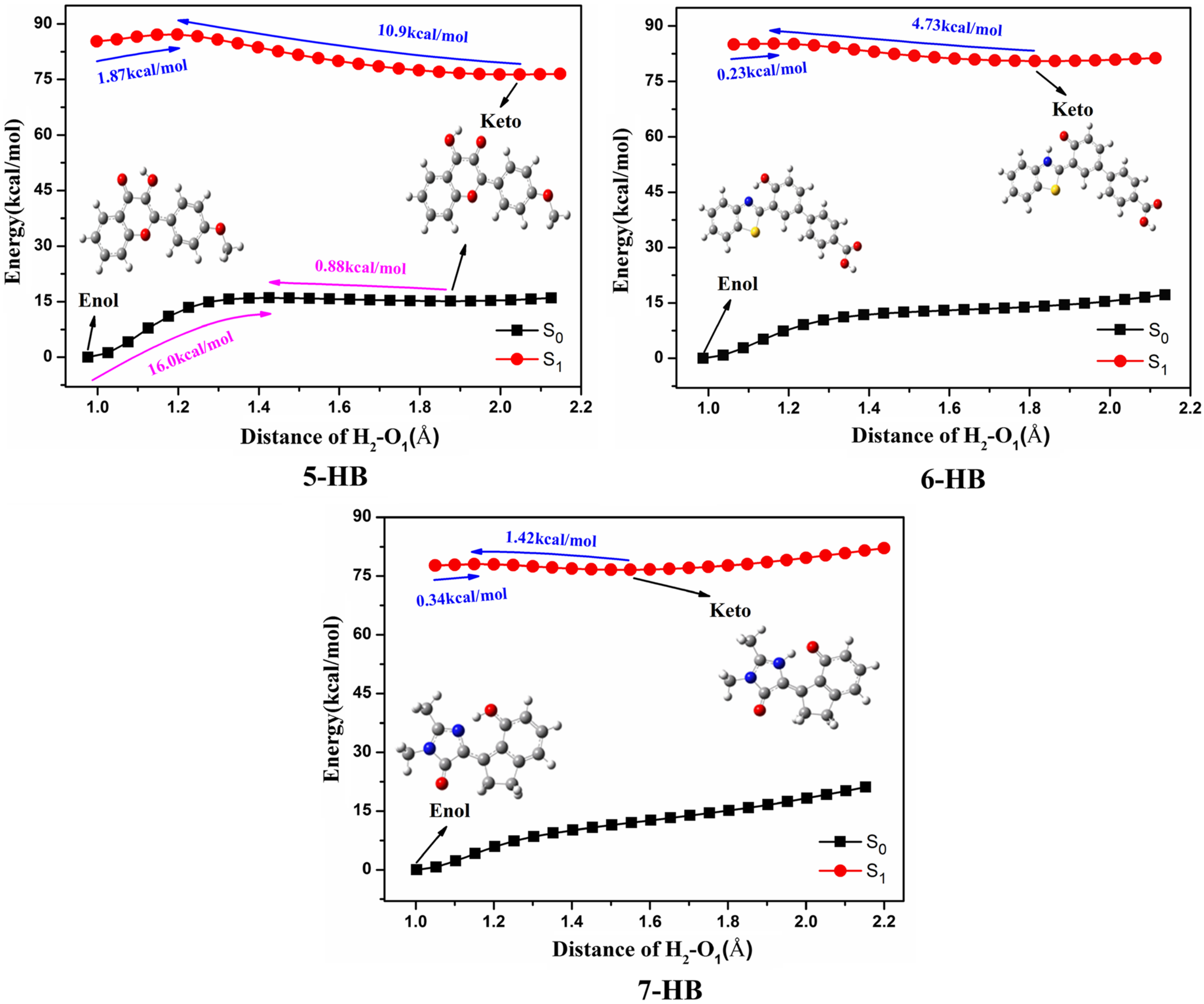

Fig. 5 Potential energy curves of 5-HB, 6-HB and 7-HB in the S_0 and S_1 states

the reverse barrier of 5-HB is very small (0.88 kcal/mol), so 5-HB is inclined to exist in the enol structure in the S_0 state. Based on the previous discussions, it can be concluded that the ability of ESIPT varies along this order: 6-HB~7-HB > 5-HB.

4 Concluding remarks

In summary, the photophysical properties and ESIPT process of 4′- methoxy-3-hydroxyflavone (5-HB), 2-(5-carboxyphenyl)-2-hydroxyphenyl) benzothiazole (6-HB) and *o*-LHBDI (7-HB) compounds in the gas phase are theoretically studied by using M06-2X and TD-M06-2X methods. The ground and excited state structural parameters and IR vibrational spectra, electronic spectra, frontier MOs and the potential energy curves are investigated to analyze the ESIPT process. The results indicate that the intramolecular H-bonds are obviously enhanced in the S_1 state based on the shortened H-bond distance and the redshift of IR vibrational frequency of O_1–H_2, which can promote the ESIPT reactions. The intramolecular H-bonds of 6-HB and 7-HB in the S_1 state are not much different, both are much stronger than that of 5-HB. The energy gap between HOMO and LUMO indicates that 7-HB has a higher chemical activity and lower kinetic stability than 5-HB and 6-HB. The calculated potential energy curves and potential barriers in the S_0 and S_1 states reveal that PT process is apt to happen in the S_1 state, and it is hard to occur in the S_0 state. The H-bonds in the six- and seven-membered ring intramolecular H-bond of 6-HB and 7-HB are stronger than that in the five-membered ring intramolecular H-bond of 5-HB, causing that the ESIPT processes of the former are nearly barrierless, but the latter needs to overcome some barriers. The ESIPT processes of 6-HB and 7-HB are much easier and faster than that of 5-HB. It is obvious that the size of intramolecular H-bonding ring may affect the ESIPT process.

Acknowledgements This work was supported by grants from the National Natural Science Foundation of China (21403114).

References

1. Shen Y, Zhang XY, Wu Y, Zhang YY, Liu XW, Chen YD, Li HT, Zhong YT (2018) Spectrochim Acta, Part A 205:66
2. Song YZ, Liu S, Ma YZ, Yang YF, Li YQ, Xu JH (2018) J Mol Struct 1173:341
3. Li XR, Ma H, Qian J, Cao T, Teng ZD, Iqbal K, Qin WW, Guo HC (2019) Talanta 194:717
4. Sheng H, Hu YH, Zhou Y, Fan SM, Cao Y, Zhao XX, Yang WG (2019) Dyes Pigments 160:48–57
5. Lan RF, Yang YF, Ma YZ, Li YQ (2017) Spectrochim Acta, Part A 183:37
6. Gomathi A, Viswanathamurthi P (2019) J Photochem Photobiol A Chem 369:97
7. Paterson MJ, Robb MA, Blancafort L, DeBellis AD (2005) J Phys Chem A 109:7527
8. Chen KY, Hsieh CC, Cheng YM, Lai CH, Chou PT (2006) Chem Commun 42:4395
9. Park SH, Kwon OH, Lee YS, Jang DJ, Park SY (2007) J Phys Chem A 111:9649
10. Luxami V, Kumar S (2012) RSC Adv 2:8734
11. Klymchenko AS, Shvadchak VV, Yushchenko DA, Jain N, Mély Y (2008) J Phys Chem B 112:12050
12. Liu B, Wang JF, Zhang G, Bai RK, Pang Y (2014) ACS Appl Mater Interfaces 6:4402
13. Julien M, Abdellah F, Mathieu C, Vérité PM, Jacquemin D, Ulrich G (2019) Dyes Pigments 160:915
14. Hu Y, Joung JF, Jeong JE, Jeong Y, Woo HY, She YB, Park SN, Yoon J (2018) Sens Actuators B Chem 280:298
15. Liu LY, Wu SS, Yu J, Chai S, Cong SL (2019) Spectrochim Acta, Part A 207:61
16. Sobolewski AL, Domcke W, Hättig C (2006) J Phys Chem A 110:6301
17. Chen KY, Cheng YM, Lai CH, Hsu CC, Ho ML, Lee GH, Chou PT (2007) J Am Chem Soc 129:4534
18. Cui G, Lan Z, Thiel W (2012) J Am Chem Soc 134:1662
19. Zhang Z, Hsu YH, Chen YA, Chen CL, Lin TC, Shen JY, Chou PT (2014) Chem Commun 50:15026
20. Lee MH, Kim JS, Sessler JL (2015) Chem Soc Rev 44:4185
21. Stasyuk AJ, Cyrański MK, Gryko DT, Solà M (2015) J Chem Theory Comput 11:1046
22. Parada GA, Markle TF, Glover SD, Hammarström L, Ott S, Zietz B (2015) Chem Eur J 21:6362
23. Wu D, Guo WW, Liu XY, Cui G (2016) Chem Phys Chem 17:2340
24. Roohi H, Nokhostin R, Mohamadnia M (2016) Dyes Pigments 134:106
25. Zhao J, Yang Y (2016) J Mol Liq 220:735
26. Li D, Liu Y (2015) J At Mol Sci 6:146
27. Zhao J, Li P (2015) Commun Comput Chem 3:66
28. Yang D, Zheng R, Wang Y, Lv J (2015) J At Mol Sci 6:197
29. Zhao J, Chen J, Cui Y, Wang J, Xia L, Dai Y, Song P, Ma F (2015) Phys Chem Chem Phys 17:1142
30. Park S, Kwon OH, Kim S, Park S, Choi MG, Cha M, Park SY, Jang DJ (2005) J Am Chem Soc 127:10070
31. Wu YK, Peng XJ, Fan JL, Gao S, Tian MZ, Zhao JZ, Sun S (2007) J Org Chem 72:62
32. Das K, Sarkar N, Ghosh AK, Majumdar D, Nath DN, Bhattacharyya K (1994) J Phys Chem 98:9126
33. Chou PT, Chen YC, Yu WS, Chou YH, Wei CY, Cheng YM (2001) J Phys Chem A 105:1731
34. Sobolewski AL, Domcke W (2007) J Phys Chem A 111:11725
35. Kanlayakan N, Kerdpol K, Prommin C, Salaeh R, Chansen W, Sattayanon C, Kungwan N (2017) New J Chem 41:8761
36. Chu Q, Medvetz DA, Pang Y (2007) Chem Mater 19:6421
37. Yang W, Chen X (2014) Phys Chem Chem Phys 16:4242
38. Li Y, Wang L, Guo X, Zhang JJ (2015) J Comput Chem 36:2374
39. Zhang W, Yan YL, Gu JM, Yao JN, Zhao YS (2015) Angew Chem Int Ed 54:7125
40. Azarias C, Budzák S, Laurent AD, Ulrich G, Jacquemin D (2016) Chem Sci 7:3763
41. Zhang D, Yang Z, Li H, Pei Z, Sun S, Xu Y (2016) Chem Commun 52:749
42. Sakai K, Tsuchiya S, Kikuchi T, Akutagawa T (2016) J Mater Chem C 4:2011
43. An B, Yuan H, Zhu Q, Li Y, Guo X, Zhang J (2017) Spectrochim Acta, Part A 175:36
44. Bardez E, Devol I, Larrey B, Valeur B (1997) J Phys Chem B 101:7786
45. Zamotaiev OM, Postupalenko VY, Shvadchak VV, Pivovarenko VG, Klymchenko AS, Mély Y (2011) Bioconjug Chem 22:101
46. Woolfe GJ, Thistlethwaite PJ (1981) J Am Chem Soc 103:6916
47. Arai T, Moriyama M, Tokumaru K (1994) J Am Chem Soc 116:3171
48. Hsieh CC, Ho ML, Chou PT (2010) Organic dyes with excited-State transformations (electron, charge, and proton transfers). In: Demchenko AP (ed) Advanced fluorescence reporters in chemistry and biology I. Fundamentals and molecular design, vol 8. Springer, Berlin, pp 225–266
49. McMorrow D, Kasha M (1983) J Am Chem Soc 105:5133
50. Sholokh M, Zamotaiev OM, Das R, Postupalenko VY, Richert L, Dujardin D, Zaporozhets OA, Pivovarenko VG, Klymchenko AS, Mély Y (2015) J Phys Chem B 119:2585
51. Kwon JE, Park SY (2011) Adv Mater 23:3615
52. Zhao J, Ji S, Chen Y, Guo H, Yang P (2012) Phys Chem Chem Phys 14:8803
53. Li K, Feng Q, Niu GL, Zhang WJ, Li YY, Kang MM, Xu K, He J, Hou HW, Tang BZ (2018) ACS Sens 3:920
54. Hsieh CC, Chou PT, Shih CW, Chuang WT, Chung MW, Lee J, Joo T (2011) J Am Chem Soc 133:2932
55. Guo ZQ, Chen WQ, Duan XM (2012) Dyes Pigments 92:619
56. Hsu YH, Chen YA, Tseng HW, Zhang Z, Shen JY, Chuang WT, Lin TC, Lee CS, Hung WY, Hong BC, Liu SH, Chou PT (2014) J Am Chem Soc 136:11805
57. Chen YA, Meng FY, Hsu YH, Hung CH, Chen CL, Chung KY, Tang WF, Hung WY, Chou PT (2016) J Chem Eur 22:14688
58. Zhao Y, Truhlar DG (2008) Theor Chem Acc 2008(120):215
59. Frisch MJ, Truck GW, Schlegel HB, Scuseria GE, Robb MA, Cheeseman JR, Scalmani G, Barone V, Mennucci B, Petersson GA, Nakatsuji H, Caricato M, Li X, Hratchian HP, Izmaylov AF, Bloino J, Zheng G, Sonnenberg JL, Hada M, Ehara M, Toyota K, Fukuda R, Hasegawa J, Ishida M, Nakajima T, Honda Y, Kitao O, Nakai H, Vreven T, Montgomery JA Jr, Peralta JE, Ogliaro F, Bearpark M, Heyd JJ, Brothers E, Kudin KN, Staroverov VN, Kobayashi R, Normand J, Raghavachari K, Rendell A, Burant JC, Iyengar SS, Tomasi J, Cossi M, Rega N, Millam JM, Klene M, Knox JE, Cross JB, Bakken V, Adamo C, Jaramillo J, Gomperts R, Stratmann RE, Yazyev O, Austin AJ, Cammi R, Pomelli C, Ochterski JW, Martin RL, Morokuma K, Zakrzewski VG, Voth GA, Salvador P, Dannenberg JJ, Dapprich

S, Daniels AD, Farkas O, Foresman JB, Ortiz JV, Cioslowski J, Fox DJ (2009) Gaussian 09. Gaussian Inc, Wallingford
60. Skilitsi AI, Agathangelou D, Shulov I, Conyard J, Haacke S, Mély Y, Klymchenko A, Léonard J (2018) Phys Chem Chem Phys 20:7885
61. Wang Y, Yin H, Shi Y, Jin M, Ding D (2014) New J Chem 38:4458
62. Wang Y, Li H, Shi Y (2015) New J Chem 39:7026
63. Adamo C, Jacquemin D (2013) Chem Soc Rev 42:845
64. Liu YH, Mehata MS, Lan SC (2014) Spectrochim Acta, Part A 2014(128):280
65. Liu Y, Ding J, Liu R, Shi D, Sun J (2009) J Photochem Photobiol, A 201:203
66. Zhao J, Song P, Ma F (2015) Commun Comput Chem 3:44
67. Zhao GJ, Northrop BH, Han KL, Stang PJ (2010) J Phys Chem A 114:9007
68. Zhao GJ, Han KL (2009) J Phys Chem A 113:4788
69. Yang Y, Liu Y, Yang D, Li H, Jiang K, Sun J (2015) Spectrochem Acta Part A 151:814
70. Fleming I (1976) Frontier orbitals and organic chemical reactions. Wiley, New York